
Article:
Nicholas, G., Mills, R., Song, W. et al. (2 more authors) (2022) Feasibility of using low-sampled accelerometer measurements for bolt joint looseness detection. IET Renewable Power Generation, 16 (13). pp. 2762-2777. ISSN 1752-1416

https://doi.org/10.1049/rpg2.12512

Received: 18 November 2021 | Revised: 4 April 2022 | Accepted: 23 May 2022

IET Renewable Power Generation

DOI: 10.1049/rpg2.12512

The Institution of Engineering and Technology WILEY

ORIGINAL RESEARCH

Feasibility of using low-sampled accelerometer measurements for bolt joint looseness detection

Gary Nicholas[1] | Robin Mills[2] | Wooyong Song[3] | Hyunjoo Lee[3] | Rob Dwyer-Joyce[1]

[1]Leonardo Centre for Tribology, Department of Mechanical Engineering, The University of Sheffield, Sheffield, UK

[2]Dynamics Research Group, Department of Mechanical Engineering, The University of Sheffield, Sheffield, UK

[3]Offshore Renewables Energy Catapult, Glasgow, UK

Correspondence
Dr. Gary Nicholas, Room E201, Sir Frederick Mappin Building, Mappin St, Sheffield, S1 3JD, UK.
Email: Gary.nicholas@sheffield.ac.uk

Funding information
Engineering and Physical Sciences Research Council, Grant/Award Number: EP/N016483/1; Powertrain Research Hub

Abstract

In this work, the feasibility of using low-sampled vibration signals for bolt joint tightness detection was investigated. Testing was carried out on multiple bolt joint configurations using a bench top electrodynamic shaker rig. Two data-processing methods were successfully used to deduce bolt joint loosening from the accelerometer measurements, namely the resonant frequency and regression methods (ARX and AR-ARX). Both methods were able to detect loosening of bolt joints, however, the latter possesses higher sensitivity in detecting the position of the loosened bolt among an array of bolts. As the resonant frequency of wind turbines is low (0.35–2 Hz), the minimum sampling rate for bolt joint tightness detection is consequently also low (twice the resonant frequency). This facilitates potential use of existing accelerometer instrumentation on wind turbines, typically sampled at low rates.

1 | INTRODUCTION

Bolted joints are widely used in structures and machinery, including wind turbines, due to their non-permanent capability. They, however, possess an inherent flaw as they are prone to self-loosening. Loosening can be defined as a subsequent loss of preload following the completion of its tightening procedure [1]. The mechanism for bolt loosening is divided into two: rotational or non-rotational loosening [2]. Rotational loosening or self-loosening occurs when the bolt rotates under the action of external loading whilst non-rotational loosening occurs during a loss of bolt preload despite no relative motion between the internal and external threads of the bolt joint. The latter can occur as a result of deformation or partial plastic collapse of the bolted interfaces during tightening, creep and thermal expansion or contraction.

For self-loosening of bolts, the most widely cited theory is that of Junker [3]. He proposed that dynamic shear loading results in far more severe loosening of bolt joints compared to axial loading and relative motion will occur when shear forces acting on the joint are larger than the frictional resistive force generated by the bolt preload. Pai and Hess [4, 5] advanced the understanding of bolt joint loosening under transverse motion. They stipulated that loosening could occur as a result of accumulation of localised slip over cyclic shear loading, even at magnitudes lower than the frictional resistive force and complete thread slip occurs before complete slip at bolt head contact. Contributions to slip were largely attributed to elastic deformation of the contacting surfaces, resulting from bending of the bolt heads due to transverse loading, variation in shear loading, and axial loading due to Poisson's ratio. Koch [6] divided the self-loosening process into four phases where the first phase is characterised by no slipping at both head and thread interfaces, the second phase occurs when the transverse force exceeds the frictional resisting force between the nut and clamped part contacts, resulting in complete slip at these interfaces and localised slip at bolt head contact. Phase three occurs when the bolt head contact transitions from partial to complete slip and for phase four, due to the continued sliding of bolt head, the bolt shank will sustain additional shear force as a result of lateral contact with the clamped part.

Shaft misalignment in machinery is undesirable as it will result in premature breakdowns, especially at the weakest link (bearings and couplings). Loose bolted joints are thought to contribute to shaft misalignment [7, 8]. In wind turbine drivetrains, the complete loosening of even 1% of drivetrain bolt joints was thought to be sufficient to induce shaft misalignment whilst also posing a health hazard. Such misalignments increase bearing loading and stresses which potentially result in off-design operation and subsequently premature bearing failures.

Various practices exist that aim to prevent self-loosening of bolted joints [9–11]. These include increasing the friction between the clamped surfaces, reducing clearance between mating components, high ratio of bolt length to bolt head diameter for misalignment compensation, high bolt joint preload and avoiding shear loading through joint reorientation.

As relative motion is necessary to induce loosening, products for preventing bolt loosening are typically designed to minimise or eliminate relative motion between the bolt joint and mating surfaces [12]. Most, however, were only able to reduce the severity of bolt loosening through preventing full detachment of nut from bolt joint. These include preload-independent locking methods (hard-lock nuts, PAL nut), free spinning preload dependant locking methods (wedge-lock and serrated face washers), prevailing torque locking methods (elliptically deformed threads, nylon inserts) and adhesive locking methods (Loctite).

In relation to monitoring of bolt joint looseness, several methods are common outside the wind industry, particularly in locomotive, subsea pipelines, and pressure vessels. These include direct measurement of bolt torque and preload [13], electrical impedance [14, 15], vibration [16–18], ultrasonic methods [19–22] as well as imaging methods [23–27]. Direct measurement of bolt torque and preload is simple and straightforward; however, it is not suitable for online monitoring due to low accuracy and human error [28]. Impedance-based methods and active piezo sensing provide better accuracy but are relatively expensive due to the large setup costs (each bolt joint required to be instrumented) as well as high sampling rates required for active piezo sensing. Imaging methods [23–27] utilise some form of image acquisition device (smart phone or charge-coupled device (CCD) camera) and post-processing (Hough transform, Canny edge detection or DIC) for detection of loosening angle to within an accuracy of ±2.6° [23] in wind turbine applications. However, the methods are limited in their measurement range from 0° to 60° [26] and it remains to be proven whether similar accuracy can be achieved in field with varying bolt dimensions and images are subjected to poor lighting, debris, presence of oil as well as vibration. On the other hand, vibration methods allow for larger coverage of bolt joint looseness detection using a single sensor. These methods [16–18] exploit the variation in resonant frequency of the structure or component as the stiffness of the structure reduces with increasing loosening of bolts. Comprehensive overviews of the existing bolt looseness detection methods can be found in [28–30].

Low-sampled vibration signals were previously used through a hybrid vibration and impedance-based method in a previous study [31]. The focus of this study is to investigate the feasibility of using low-sampled vibration signals (20—2000 Hz) to detect bolt loosening through three methods, namely the resonant frequency, ARX and AR-ARX linear regression methods. The latter two are of completely different approaches compared to the hybrid method [31]. One potential application would be in wind turbines where active monitoring of bolt joint looseness is uncommon and existing practices (manual inspection, maintenance) are time-consuming, costly, and demanding due to the large number of bolted joints and accessibility issues especially for remote offshore wind turbines.

2 | METHODOLOGY

2.1 | Electrodynamic shaker rig

Figure 1 shows a photo and schematic of the test setup for the electrodynamic shaker testing. The assembly shown in the figure consisted of stanchions and plates with 10 M6 bolts at the centre. Axial vibration was applied by the electrodynamic shaker onto the test assembly to simulate vibrations sustained by bolts during operational condition. Three accelerometers were used, one attached onto the shaker test bed, whilst the other two were positioned on the test plate. The shaker bed accelerometer provided input measurement whilst output measurements were obtained from the test plate. The additional accelerometer on the test plate was for control of the electrodynamic shaker excitation.

Initially, to measure the frequency response of the assembly, simple static tap tests were performed. This also facilitated the selection of appropriate excitation frequency for the dynamic shaker tests. The procedure for the static tap test is outlined below:

1. The test assembly was assembled onto the shaker bed alongside a single accelerometer positioned on the test plate for measurement.
2. The test plate was struck 10 times with a metal rod at various loosening conditions (sequentially loosening bolts, varying bolt torque, different loose bolt patterns).
3. The first loosening condition involved sequentially loosening a single bolt starting from the outer left bolt to the outer right bolt.
4. The second loosening condition involved initially loosening the inner left and right bolts, followed by the outer bolts, and finally varying the torque on the centre bolt until fully loosened.
5. For the third loosening condition, the centre bolt was fully loosened, followed by the inner left bolt and subsequently both centre and inner left bolts.
6. Accelerometer measurements in time domain were captured as the test plate was struck at each stage of loosening and

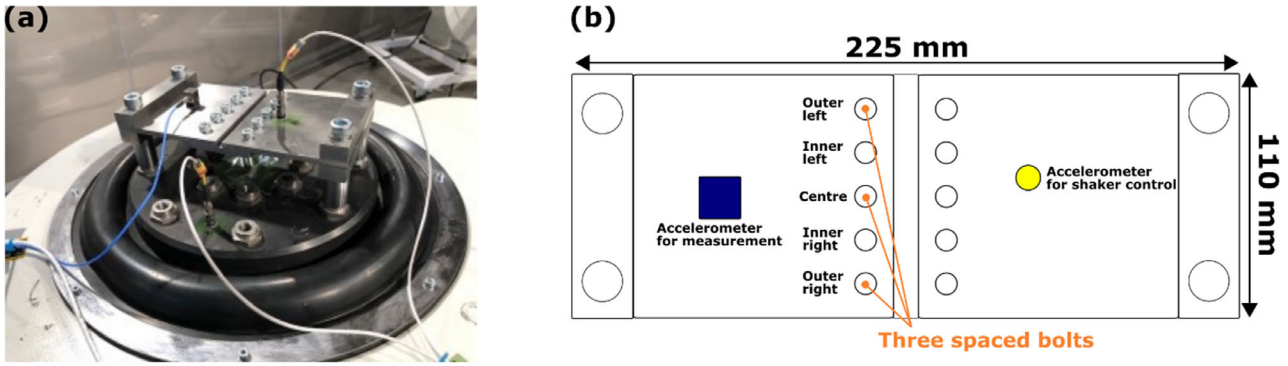

FIGURE 1 (a) Photo and (b) schematic of electrodynamic shaker testing setup

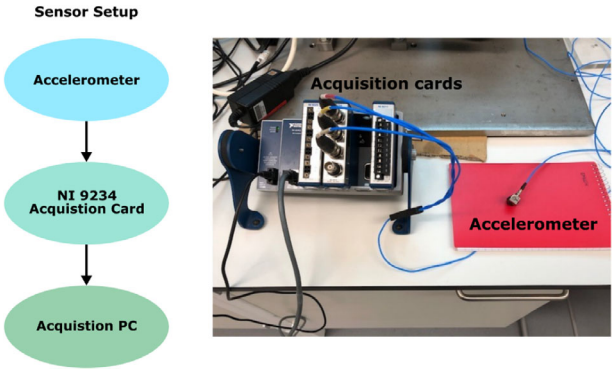

FIGURE 2 Sensor arrangement schematic and photo

converted into the spectral domain. Measurements were sampled at 10.24 kHz.

7. Measurements were subsequently analysed in the spectral domain through Fast Fourier Transform (FFT).

The procedure for dynamic shaker tests does not differ from previously outlined for static tap tests except in this case, measurements were taken when the shaker table was vibrated under sweep excitation between 200 and 1200 Hz, and at different sampling rates and is outlined below:

1. Test assembly was assembled onto the shaker bed alongside three accelerometers with one positioned at the shaker bed and the other two on the test plate.
2. A sweep excitation between 200 and 1200 Hz was applied to the structure with constant power of 0.01 G^2/Hz at first and second loosening condition.
3. Accelerometer measurements in time domain were acquired at minimum and maximum hardware sampling rates (2.04 and 51.2 kHz) for each stage of loosening, for sensors positioned at shaker base (input) and test specimen (output).

2.2 | Sensor arrangement and acquisition

Figure 2 shows a schematic and photo of the data acquisition hardware and sensor used to capture vibration measurements. The accelerometer used was a PCB 356B21 triaxial accelerometer with a frequency range up to 7 kHz for the x-axis and 10 kHz for the y and z-axis.

The sensor was connected to an NI-9234 acquisition card and the data processing was carried out using LabVIEW. The NI acquisition card has a minimum and maximum sampling rate of 2.04 and 51.2 kHz. Measurements were taken at minimum and maximum sampling rate to test the influence of sampling rate on the accuracy of bolt loosening detection algorithms.

2.3 | Methods for bolt looseness detection

In this study, two processing methods were used to infer bolt loosening, namely the resonance frequency and regression method [14]. These are detailed below:

2.3.1 | Resonance frequency method

All structures exhibit a frequency at which when excited will vibrate at a higher amplitude. This occurs at the resonant frequency of the structure. The resonant frequency, f_{res} is affected by the mass, m and stiffness, k of the structure as mathematically described in Equation (1). As the number of loosened bolts increase or the tightness of the bolt joints decrease, the structure will experience a reduction in stiffness. This will result in a reduction in the resonance frequency of the structure. As such, through measuring the resonance frequency of a structure, bolt joint tightness can be determined. The full data processing routine for the resonance method is detailed in Section 3.1.

$$f_{\text{res}} = \frac{1}{2\pi}\sqrt{\frac{k}{m}}. \tag{1}$$

2.3.2 | Regression method

The regression method used for bolt detection was adapted from [14]. These are time-series techniques and are an alternative to the resonant frequency approach. Both regression

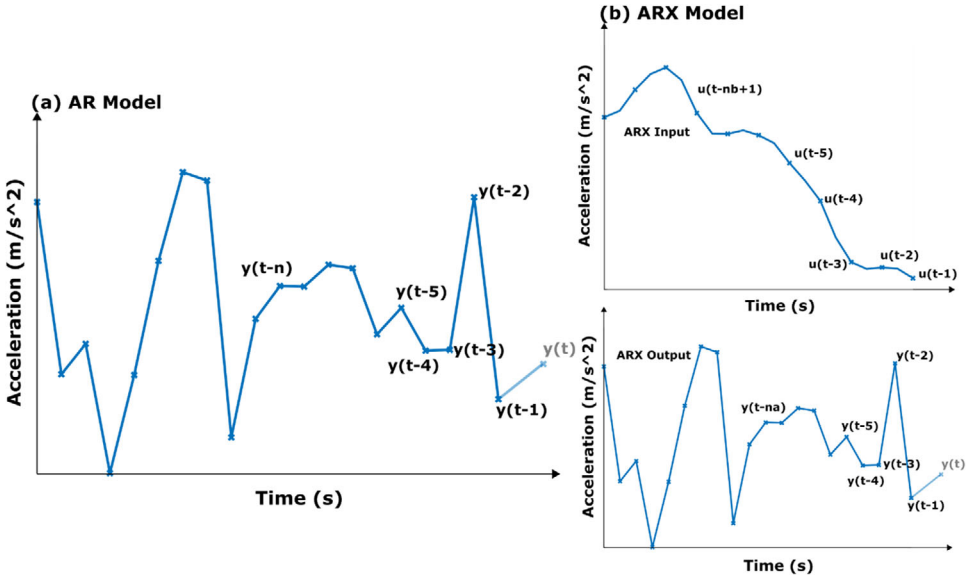

FIGURE 3 Notation employed in the (a) autoregressive (AR) and (b) autoregressive with extra input (ARX) model plotted using dummy datapoints

methods employ the standard deviation ratio of the residual errors as damage sensitive parameters to monitor bolt joint looseness. Such methods have been previously used for structural health monitoring in both real-life [32] and experimental applications [33]. For this study, both ARX and AR-ARX models were used to derive a damage characteristic parameter, D_F, which was subsequently used to provide an indication of bolt/structure loosening.

AR model

An autoregressive (AR) model predicts or forecasts the variable of interest, $y(t)$ through a linear combination of past values of the variable, $y(t-n)$. In this study, the variable of interest is the vibration response of the system. The term 'auto' within the name refers to regression of the variable against itself and the mathematical form is shown in Equation (2) where a_n are the regression parameters and n is the model order. $e(t)$ is the residual of the model which has zero mean, variance and is uncorrelated in the time domain (white noise). Figure 3 illustrates the notation employed for the model constructed using dummy datapoints. A one-order AR model would only be built using a single past value, $y(t-1)$ with regression parameter a_1, a two-order model with two, $y(t-1)$ and $y(t-2)$ and regression parameters a_1 and a_2 and so on.

$$y(t) + a_1 y(t-1) + \cdots + a_n y(t-n) = e(t). \tag{2}$$

Equation (2) can be rewritten as

$$A(q)\, y(t) = e(t), \tag{3}$$

$$A(q) = 1 + a_1 q^{-1} + \cdots + a_n q^{-n}, \tag{4}$$

where q^{-1} is the delay operator such that

$$u(t = 1) = q^{-1} u(t). \tag{5}$$

Subsequently, $A(q)$ can be estimated through least square identification as detailed in [34, 35].

ARX model

An autoregressive with extra input (ARX) model forecasts future values with a combination of both past input and output measurements and is described in Equation (6), where $u(t-nk)$ and $y(t-na)$ are the input and output measurements, a_i and b_j their regression parameters, $e(t)$ the residual error, na and nb are the model orders and nk is the time delay between the output, $y(t)$ and input, $u(t)$. In this study, the input measurements, $u(t)$ refer to vibration signals obtained from the electrodynamic shaker bed while the output measurements, $y(t)$ are vibration responses captured from the test plate.

$$y(t) + a_1 y(t-1) + \cdots + a_{na} y(t-na) = b_1 u(t-nk) + \cdots + b_{nb} u(t-nb-nk+1) + e(t). \tag{6}$$

The polynomial representation of Equation (6) is given by

$$A(q)\, y(t) = B(q)\, u(t-nk) + e(t), \tag{7}$$

where $A(q)$ and $B(q)$ are given below and again estimated through least square method [34, 35].

$$A(q) = 1 + a_1 q^{-1} + \cdots + a_{na} q^{-na}, \tag{8}$$

$$B(q) = b_1 + b_2 q^{-1} + \cdots + b_{nb} q^{-nb+1}. \tag{9}$$

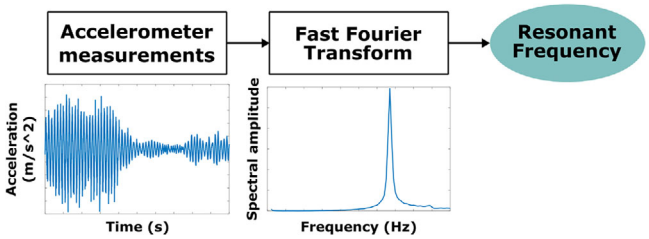

FIGURE 4 Processing routine to obtain system resonant frequency

For the ARX modelling method, input and output measurements from an unloosened structure were used to build the model and their reference residual established. The model built was subsequently used to predict or model output responses, using input measurements captured at various loosened state of the structure. The residuals, $e(t)$ were obtained by computing the difference between the measured output with the modelled output. As the model is unable to construct the residual component, $e(t)$ if the measurement residual, $e_d(t)$ is higher than the reference residual, $e_u(t)$ the system is likely to experience some degree of loosening [14]. The damage characteristic parameter, D_F is thus defined based on the reference residual, $e_u(t)$ and measurement residual, $e_d(t)$ as shown in Equation (10), where σ refers to the standard deviation (stdev) of the parameter [14]. The full processing routine for ARX regression method is detailed in §3.2.

$$D_F = \frac{stdev\,(e_d)}{mean\,(stdev\,(e_u))}\,. \tag{10}$$

AR-ARX method

As input accelerometer measurements are not typically available in field measurements, an alternative is necessary. This is known as the AR-ARX method. For this method, output vibration measurements of the test structure from unloosened states were initially used to generate AR models using Equation (7). The AR models were subsequently used to generate predictions based on the output measurements. Those predicted measurements were used as input for the ARX model and the residual from the ARX model were used to calculate the damage characteristic parameter, using Equation (10). The full processing routine for AR-ARX regression methods is detailed in §3.3.

3 | DATA-PROCESSING ROUTINE

3.1 | Resonance method

The processing routine implemented to determine resonant frequencies is straightforward (Figure 4). Measurements acquired in time domain were initially converted into frequency domain through FFT. The peak frequency that corresponds to the resonant frequency of the system is subsequently identified for each stage of loosening.

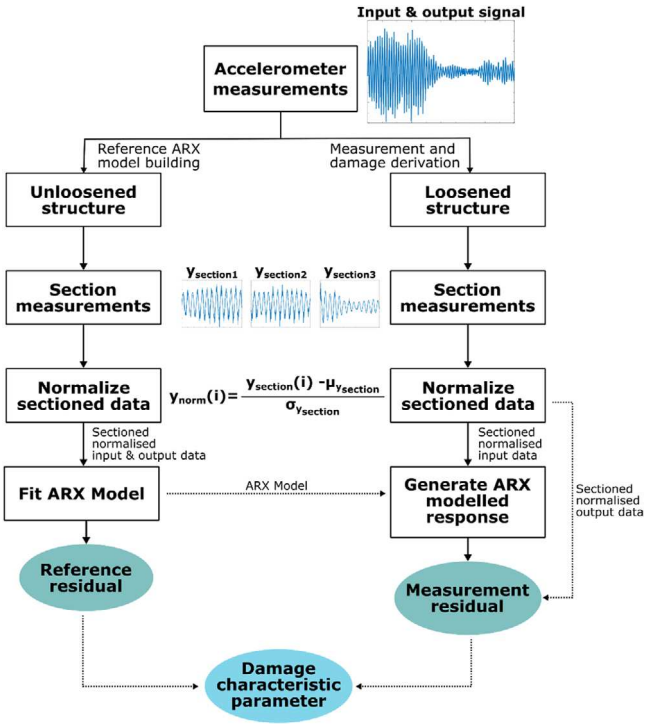

FIGURE 5 Processing routine for ARX regression method to get D_F

3.2 | ARX regression method

Regression methods outlined in the subsequent sections are more complicated with additional steps required and higher demand in computational power. Figure 5 summarises the data processing steps for the ARX regression method. The method is divided into two segments: reference model building and measurement and damage derivation. Initially, input and output measurements were obtained from the structure under an unloosened condition. The input in this case is the vibration measurements obtained from the shaker bed and the output is the vibration measurements obtained from the test plate/structure. The measured input and output signals were subsequently divided into sections containing equal amounts of datapoints, discarding the final data section if necessary. The data sections, x_{ds} were subsequently normalised with their respective mean, $\mu_{x_{ds}}$ and standard deviation values, $\sigma_{x_{ds}}$ based on Equation (11). After normalisation of data sections, an ARX model was fitted across each data sections and the reference residuals were obtained.

$$y_{\text{norm}}\ (i) = \frac{y_{\text{section}}\ (i) - \mu_{y_{\text{section}}}}{\sigma_{y_{\text{section}}}}\,. \tag{11}$$

After building the reference ARX model, accelerometer measurements were obtained from the same structure under various degree of loosening as detailed in §2.1. The input and output measurements were subsequently divided again into sections containing equal amount of datapoints and normalised using Equation (11). The ARX reference model previously built was

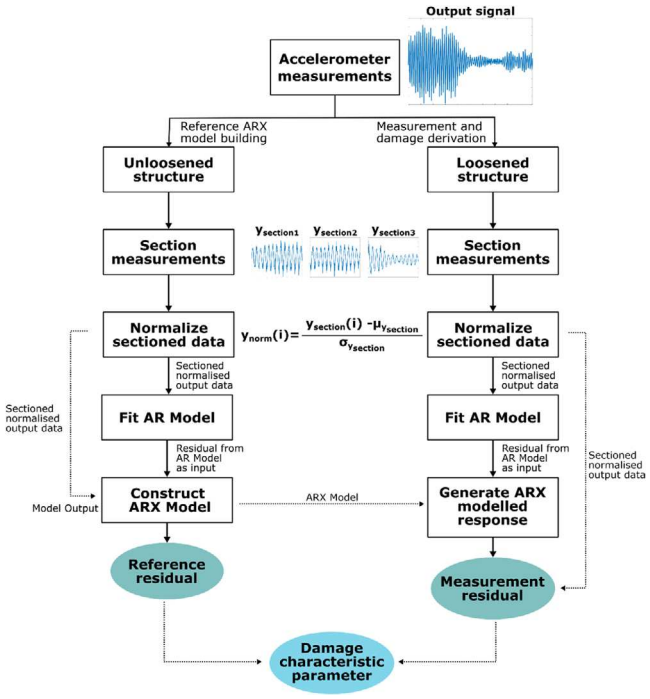

FIGURE 6 Processing routine for AR-ARX regression method to get D_F

then used alongside the input measurement from loosened condition to generate a modelled response. The measurement residuals were subsequently computed through finding the difference between output accelerometer measurements and the modelled response. Finally, the damage characteristic parameter, D_F was calculated through Equation (10). For the ARX method, an ARX (60,60) model was used with 2048 datapoints in a section. Experiments were conducted under controlled conditions to limit the influence of environmental conditions (temperature and humidity) on the accelerometer measurements. Apart from that, a normalisation procedure was carried out on the accelerometer measurements to further limit environmental influences [18, 32–33]. The division of the full data length into sections may contribute to maintaining signal input stationarity. Apart from that, the step improves the accuracy of the bolt joint looseness detection through monitoring the mean and standard deviation of the damage characteristic parameter, D_F as opposed to only a single value of D_F if the data was not sectioned.

3.3 | AR-ARX regression method

Accelerometer measurements in the field often only facilitate for measurement of output vibrational responses as input signals to the system and difficult to quantify consistently. As such this exposes a weakness of the ARX regression method as it requires an input response. This, however, can be alleviated through using the AR-ARX regression method. Figure 6 shows the data processing routine for the AR-ARX regression method. Again, the processing is divided into two phases, reference ARX model building and measurements and damage derivation. The initial steps of the model building do not differ from the ARX regression method apart from only output measurements were utilised. The output response captured from the unloosened structure were divided into sections of equal data points and normalised. An AR model was subsequently fitted for each of the data sections and the resultant residuals from subtracting the measured data with the modelled data was used as input to construct an ARX model, with the measured data as the output signal. The ARX model was subsequently used to generate a set of modelled data and the reference residuals were obtained by subtracting the measured data with the modelled data for each of the data sections. After building the ARX model, output measurements captured from the structure with varying degree of loosening were divided into data sections of equal length, normalised, and fitted with an AR model to obtain the modelled data. The residuals again were used as input measurements to feed into the ARX model previously built using the unloosened data captured. Finally, the residual from the ARX model was obtained and the damage characteristic parameter was calculated using Equation (10) for each of the loosened state. For the AR-ARX method, an AR (200) and ARX (60,60) was used with a data section length of 2048. Experiments were again conducted under controlled conditions to limit the influence of environmental conditions (temperature and humidity) on the accelerometer measurements. Apart from that, a normalisation procedure was also carried out on the accelerometer measurements to further limit environmental influences [18, 32, 33].

3.4 | Static tap tests

Figure 7 shows the variation in frequency response of the test plate as the bolts were sequentially loosened from outer left to outer right. The peak within the frequency response plot corresponds to the resonance frequency of the system. As expected, the system resonant frequency is seen to decrease from around 640 Hz at its unloosened state down to 260 Hz with increasing number of loosened bolts as the stiffness of the system decreases.

Figure 8 shows the frequency response of the system as the inner bolts (centre, inner left, centre and inner left) were loosened. This was aimed to assess the sensitivity of the resonance frequency method in locating the loosened bolt within an array of bolts. When only a single bolt was loosened (centre, inner left) with the rest fully torqued up at 19 Nm, the system resonant frequency remained at 640 Hz and did not exhibit a change. However, when two inner bolts were loosened (centre and inner left), a 10-Hz reduction in the system resonance frequency was observed. Thus, the resonance frequency method is only sensitive enough to detect loosening of two or more inner bolts (centre and inner left).

Figure 9(a) shows the variation in system resonant frequency as the tightening torque for the centre bolt increases whilst Figure 9(b) shows the variation in system resonant frequency with no bolts, inner left and right bolts removed, and all bolts tightened. System resonant frequency was seen to increase with

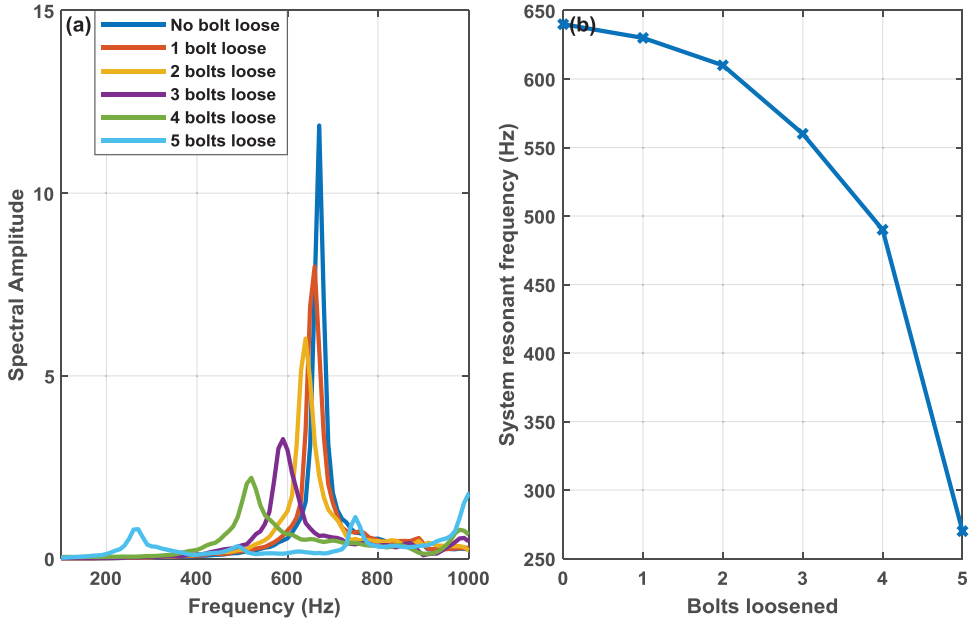

FIGURE 7 (a) Frequency response of system. (b) Variation of system resonant frequency with number of loosened bolts

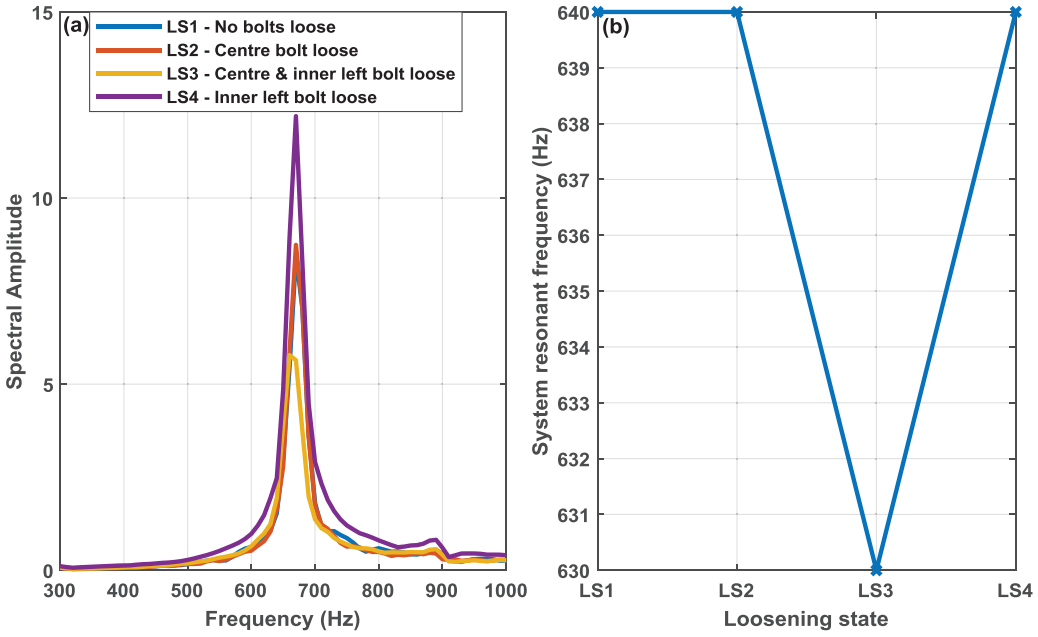

FIGURE 8 (a) Frequency response of structure (b) variation in system resonant frequency with loosening state (LS) of structure

increasing bolt tightening torque. The resonance frequency, however, does not record a significant change for tightening torques greater than 4 Nm, potentially due to the sensitivity limit of the method. The method was also unable to distinguish between fully tightened bolt arrangement against an equally spaced bolting pattern (inner left and right bolts removed). Thus, the system resonant frequency can be used to identify loosening of fully, but neither partially loosened bolt joints nor the position of loosened bolts in an array.

3.5 | Dynamic Shaker tests

3.5.1 | Resonance method

Figure 10 shows the system acceleration response in time and frequency domain captured when the unloosened structure was subjected to dynamic vibrational response. The peak within the spectral domain corresponds to the resonance frequency, observed at around 650 Hz.

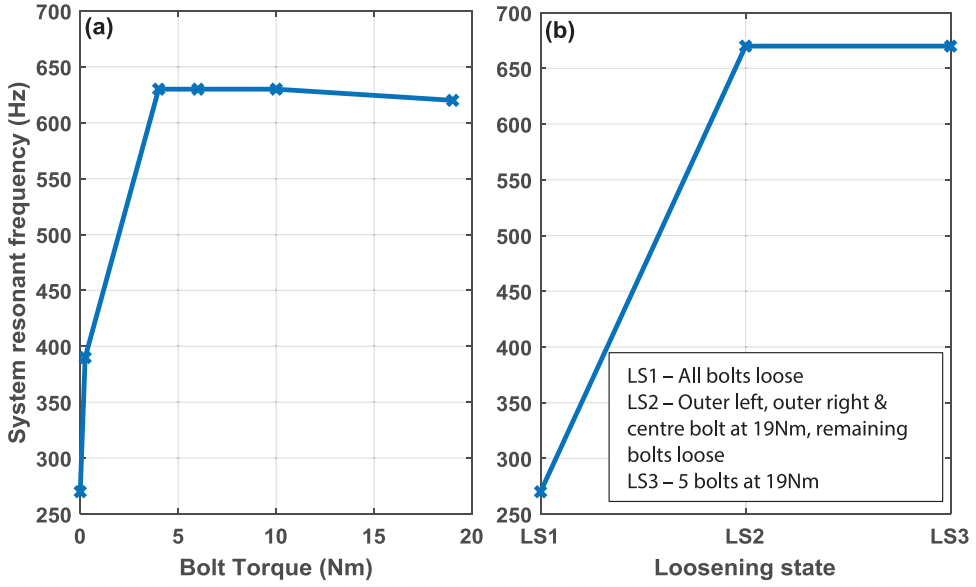

FIGURE 9 Variation of system resonant frequency with (a) bolt torque and (b) loosening state

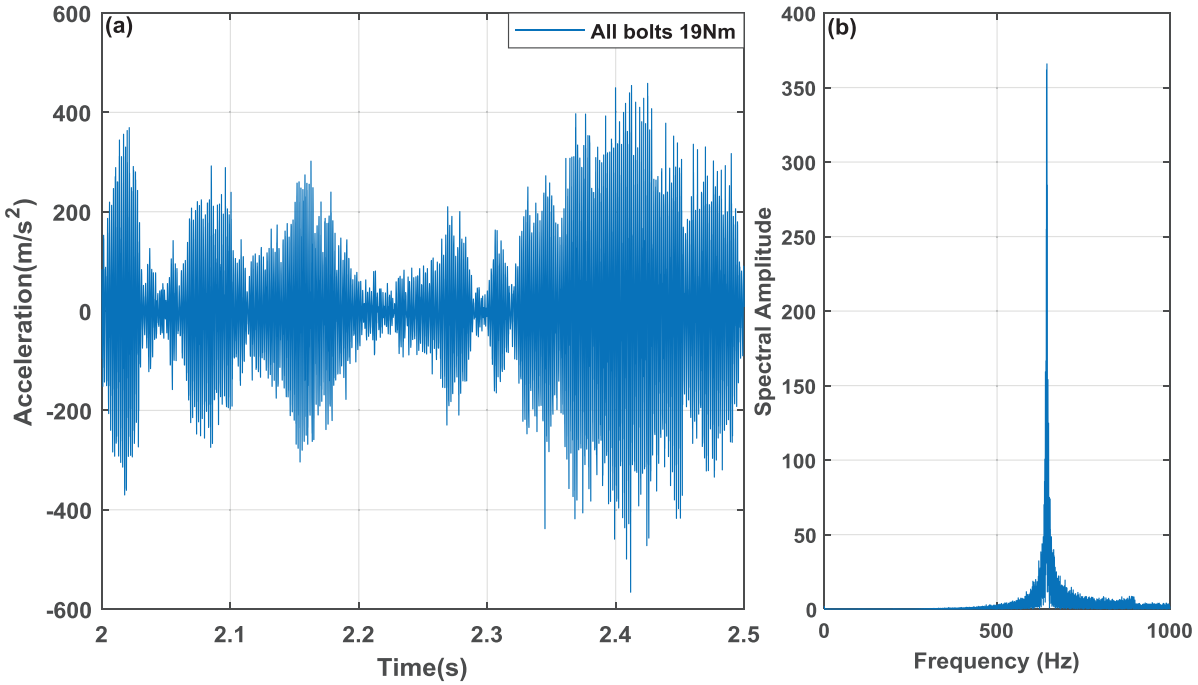

FIGURE 10 Acceleration measurement in (a) time and (b) frequency domain captured at unloosened state

As the number of bolts were sequentially loosened from outer left to outer right, the resonance frequency decreases. This is evident in Figure 11(a) where a decrease in resonant frequency of 140 Hz was observed as the structure reduced in stiffness due to reducing number of tightened bolts. Measurements were acquired at 51.2 kHz, well above the Nyquist limit of around 1.28 kHz. When the centre bolt was loosened with the remaining bolts tightened, an increase in resonant frequency was observed as shown in Figure 11(b). However, when two inner bolts were loosened (centre and inner left bolt) with the remaining bolts tightened, the resonant frequency decreased slightly, similar to the findings observed from the tap tests in Figure 8. This implies that the method is not sufficiently sensitive to detect loosening of centre bolts.

Figure 12 shows the variation in resonant frequency with various degree of structure loosening. Measurements were captured at both low and high sampling rates of 2.04 kHz and 51.2 kHz. A downward trend can be observed for the resonant frequency

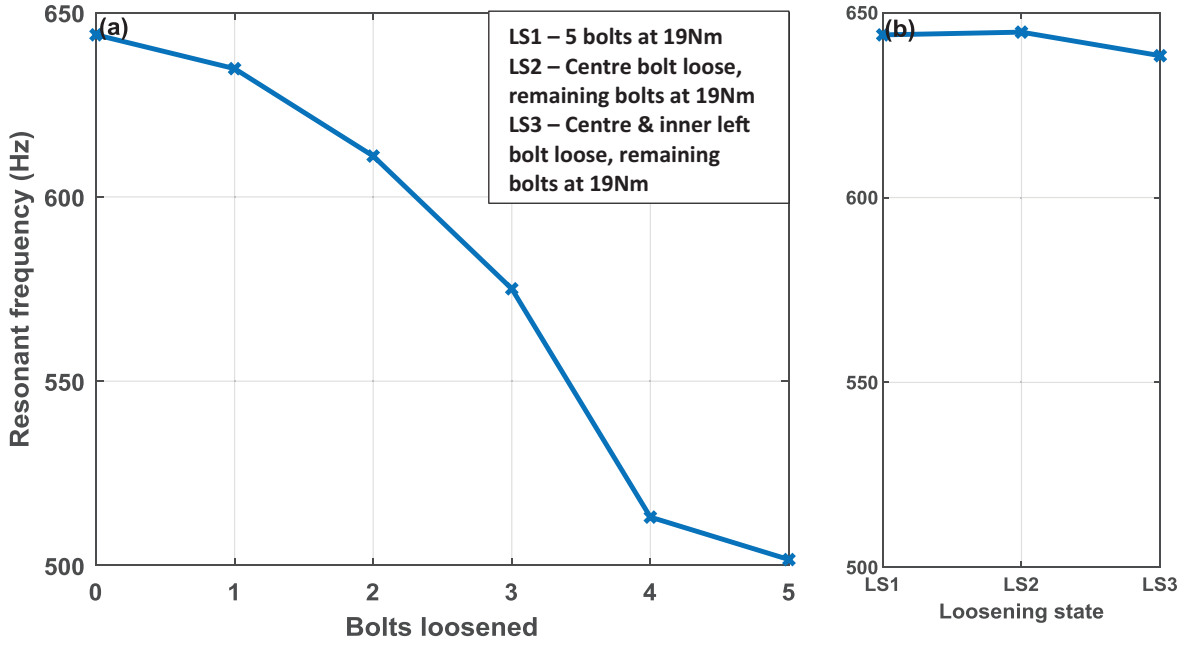

FIGURE 11 Variation in system resonant frequency with increasing number of tightened bolts

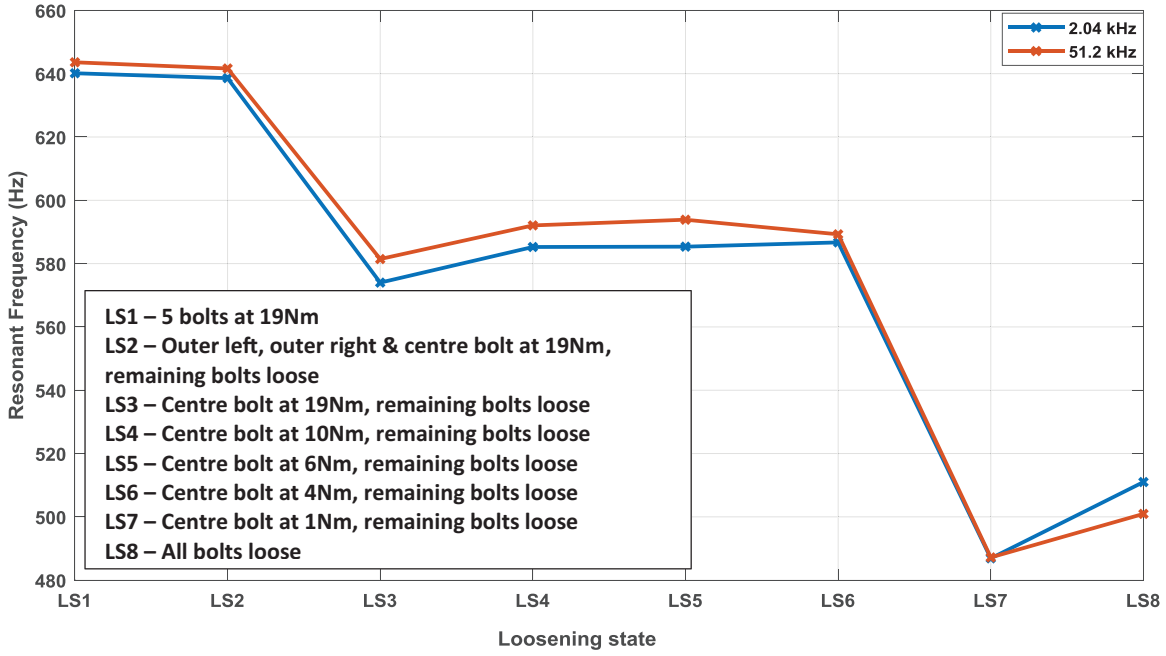

FIGURE 12 Variation in system resonant frequency with structure loosening state

as the degree of severity of the structure loosening increases. As expected, no significant differences exist between the low and high sampled results as both sampling rates exceed the Nyquist limit of 1.28 kHz. The method, however, was insensitive to centre bolt tightening torques of 4–19 Nm.

To illustrate the effect of sampling below the Nyquist limit of the measured system's resonant frequency, data acquired at 51.2 kHz were resampled at lower rates between 256 and 51.2 kHz. The results are illustrated in Figure 13. As expected, sampling rates lower than twice the resonant frequency at unloosened states (1.28 kHz) were unable to accurately determine the system resonant frequency. Measurements sampled at a higher rate than this threshold showed little to no variation. Thus, the minimum sampling rate necessary to detect bolt loosening using the resonant frequency method would be twice the resonant frequency of the unloosened structure.

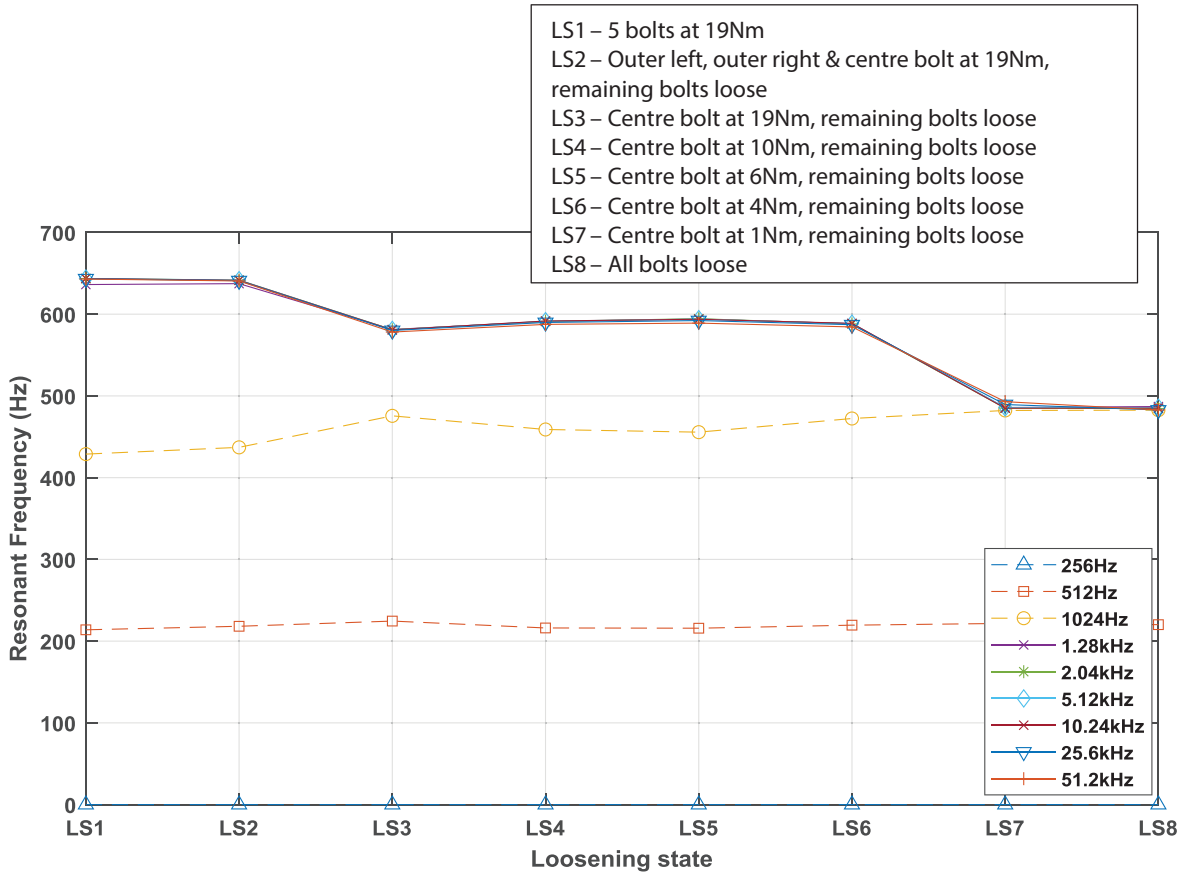

FIGURE 13 Variation in system resonant frequency with structure loosening state, and a range of sampling values

3.5.2 | ARX regression method

Figure 14 shows the change in mean and standard deviation of damage characteristic parameter, D_F as defined in Equation (10), as the number of bolted joints on the test plate were sequentially loosened from outer left to outer right (Figure 14(a) and (c)) and number of centre bolts were loosened (Figure 14(b) and (d)). Measurements were taken at 51.2 kHz. Apart from the fully loosened mean damage characteristic parameter, D_F in Figure 14(a), all the mean and standard deviation increased as the number of tightened bolts decreases. Mean and standard deviation of damage characteristic parameter, D_F also increased when the centre bolt and centre and inner left bolts were loosened, indicating a higher sensitivity for the ARX regression method as opposed to the resonance frequency method.

Both the ARX regression method and the resonance frequency method were able to detect bolt joint looseness when the bolts were sequentially loosened from outer left to outer right, however, only the ARX regression method can detect loosening of centre bolts.

Figure 15 shows the variation in mean and standard deviation of the damage characteristic parameter, D_F obtained as the structure was gradually loosened, sampled at 2.04 and 51.2 kHz. For measurements sampled at 2.04 kHz with reducing bolt tightening torque (Figure 15(a) and (c)), an increasing trend was observed for both the mean and standard deviation of D_F as the bolt tightening torque decreases, with a clearer increase evident in the mean (Figure 15(a)). For the measurements sampled at 51.2 kHz, the mean D_F was not able to distinguish bolt tightening torques between 4 and 19 Nm. An upward trend was, however, still visible for the standard deviation of D_F as the structure was gradually loosened, as shown in Figure 15(d).

It is prudent to note that to capture the amplitude peaks in time domain, a sampling rate which is 10 times the highest frequency of interest is necessary whilst a sampling rate twice the highest frequency of interest is necessary to obtain the correct spectral amplitude. If the accelerometer measurements were sampled at a lower rate, information pertaining to the system resonant frequency might not be captured within the low-sampled time series and as such the regression method will not work in detecting bolt joint looseness. To demonstrate this, data captured at 5.12 kHz was resampled at 256, 512 and 1024 Hz and the mean and standard deviation of D_F was computed for various degree of structure loosening. Results are shown in Figure 16.

For the resampled measurements at 256 and 512 Hz, the method was able to detect when the structure's inner left and right bolts were loosened (three Bolts 19 Nm) from an unloosened state, but failed to differentiate subsequent structure loosening, as the mean and standard deviation of D_F

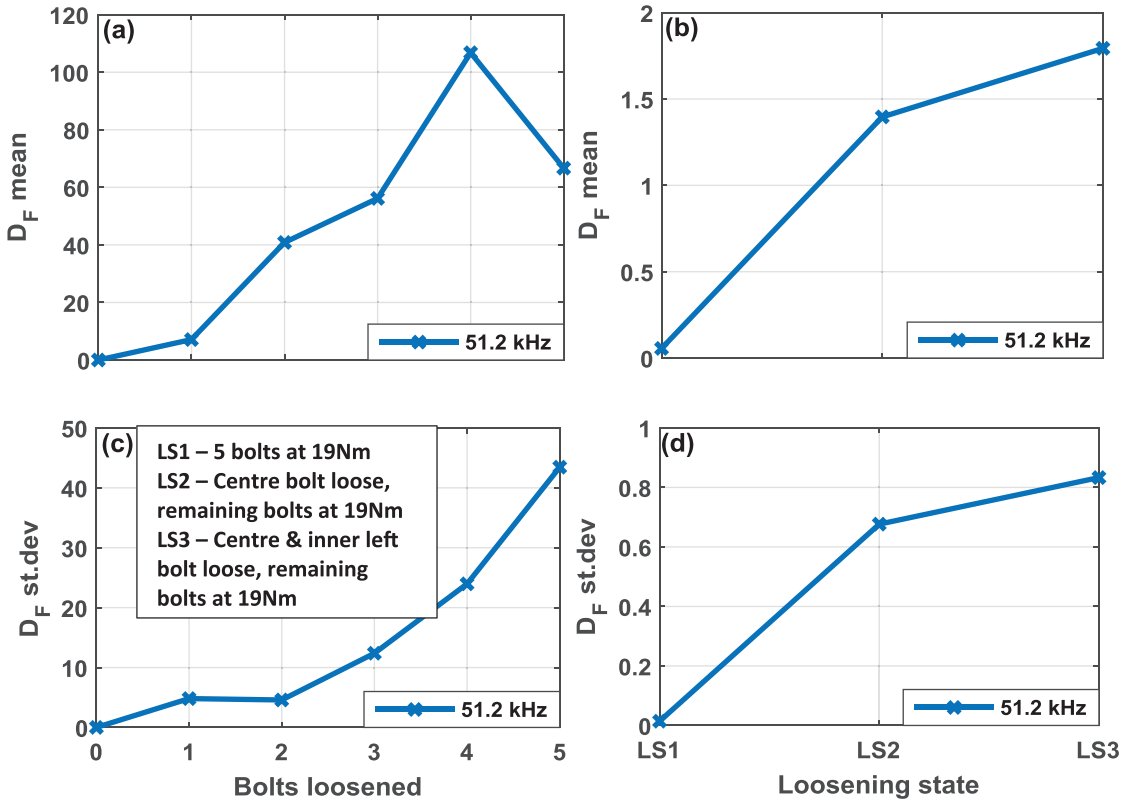

FIGURE 14 (a) and (b) Mean and (c) and (d) standard deviation of damage characteristic parameter, $\boldsymbol{D_F}$ for various degree of structure loosening, sampled at 51.2 kHz, derived through the ARX model

plateaus. For the measurement resampled at 1024 Hz shown in Figure 16, the method was able to distinguish structures with fully loosened bolts, evident from the increase in mean and standard deviation of D_F for the first two structure loosening states. However, the method was again unable to distinguish between bolt tightening torques of 4 Nm to 19 Nm. This potentially is due to the dataset used as the measurements sampled at 2.04 kHz (shown in Figure 15) was able to differentiate between different bolt torques. As such, a sufficient sampling frequency at least twice the structure's resonance frequency is still necessary for detection of bolt loosening using both ARX and also the AR-ARX method, since both detection methods are based on the same principles in detecting the change in residual as a result of bolt loosening, which results in structural stiffness reduction.

3.5.3 | AR-ARX regression method

Figure 17 shows the mean and standard deviation of D_F again for various degree of structure loosening, derived through AR-ARX method and sampled at 2.04 and 51.2 kHz. An increasing trend can be observed again for the mean and standard deviation of D_F and measurements were very similar to those derived from the ARX method as shown in Figure 15, demonstrating that both methods yield similar results despite the AR-ARX method uses only output measurements.

Figure 18 shows the variation in mean and standard deviation of D_F as the number of bolts were sequentially loosened from outer left to outer right bolts (Figure 18(a) and (c)) and also where the centre bolts were loosened (Figure 18(b) and (d)). Measurements were acquired at 51.2 kHz. As observed in Figure 14, apart from the fully loosened mean D_F in Figure 17(a), all the mean and standard deviation of D_F increased with increasing structure loosening. This also applies to when the centre bolt and centre and left bolt were loosened, demonstrating that the AR-ARX method has similar sensitivity to the ARX method in detection of centre bolt loosening, which the resonance method failed to achieve.

4 | DISCUSSION

The paper explores the capabilities and limitations of low-sampled vibration signals to detect bolt joint looseness through three methods, namely the resonant frequency and regression (AR and AR-ARX) methods through bolt loosening experiments conducted with vibration signals sampled at various rates (1.024–51.2 kHz). ARX regression method is favoured over multi-variate regression approaches in this study as the

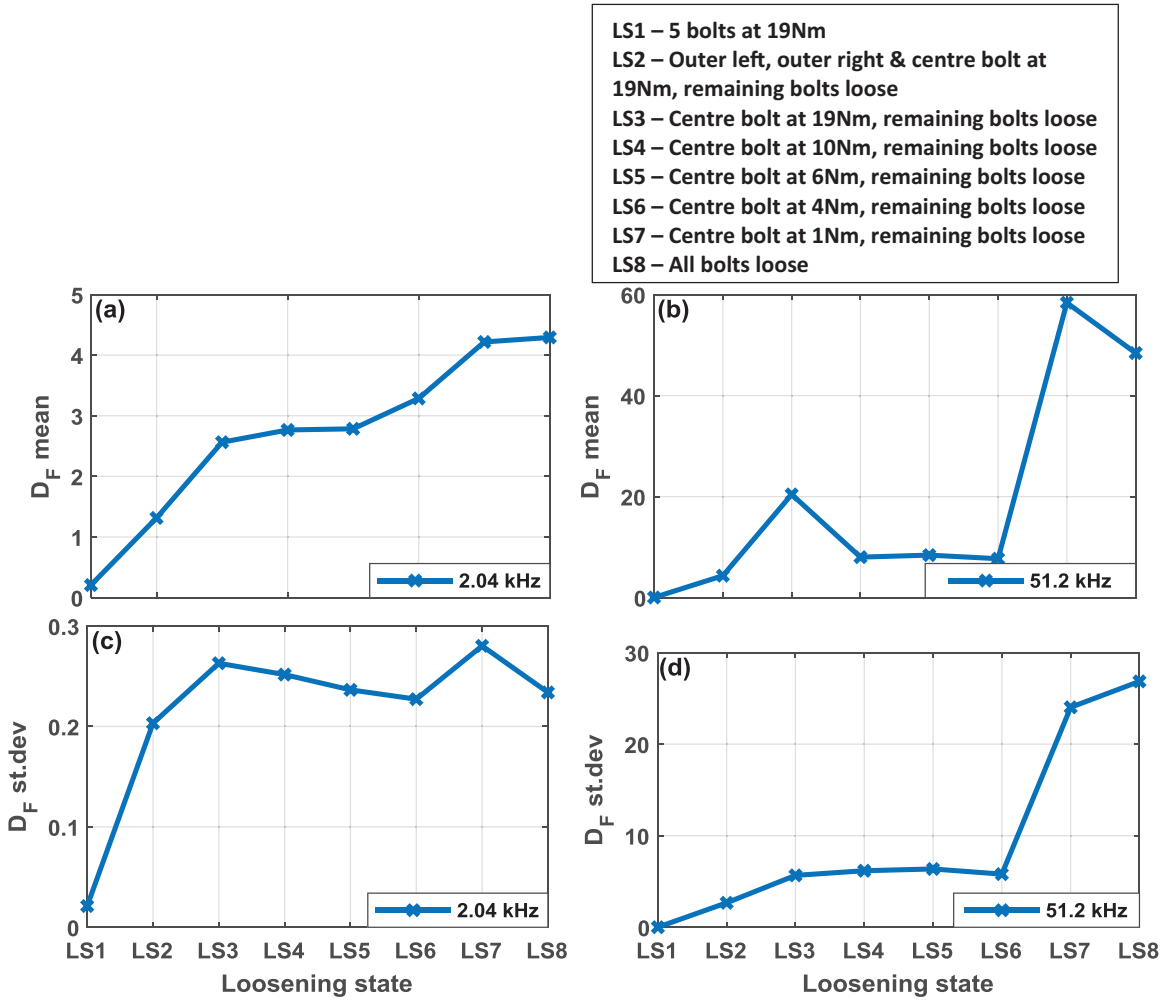

FIGURE 15 (a) and (b) Mean and (c) and (d) standard deviation of damage characteristic parameter, D_F for various degree of structure loosening, sampled at 2.04 and 51.2 kHz, derived through the ARX model

modelled data (time series vibration measurements) are dependent on past values in time.

The resonant frequency method, although having limitations in sensitivity, was proven to be able to detect bolt joint looseness within a structure. Its advantages lie in the simplicity of the method and data-processing steps required, provided that the data used are sampled at twice the frequency of interest. The method, however, is unable to detect bolt loosening of centre bolts within the structure. As such, applicability of the resonance method is limited to structures with single or double bolt arrangement or bolt arrangement with sufficiently wide separation between the bolts and thus can be applied for localised monitoring of individual main bolted joints of the wind turbine gearbox.

The two univariate regression methods trialled (ARX and AR-ARX methods) extended the detection capabilities with increased sensitivity, allowing for detection of centre bolt looseness. Thus, the regression methods are more suitable for monitoring of assemblies with multiple bolted joints such as the single or double row bolts arranged around the circumference of the wind turbine main bearing and gearbox casing. However, this comes at the cost of increased processing complexity and computation power. A crucial step in yielding good results is the building of the regression models using reference measurements obtained from an unloosened structure. This included the procedure of sectioning the reference data into appropriate number of datapoints, normalising the data sections to ensure its stationarity, and selection of appropriate model order. Models with a better fit generally would result in more accurate bolt loosening detection. In this work, the length of sectioned data and the model order were optimised through reducing Akaike's Final Prediction Error (FPE) to increase fit percentage of the model.

The sampling rate of the accelerometer measurements, as shown in Figures 13 and 16, is also crucial in the detection of bolt loosening through all three methods (resonance, ARX and AR-ARX). To fully capture all the peaks and trough in the time domain measurement, a frequency greater than 10 times the frequency of interest is required to be implemented, whereas for full quantification of the spectral domain, a frequency greater

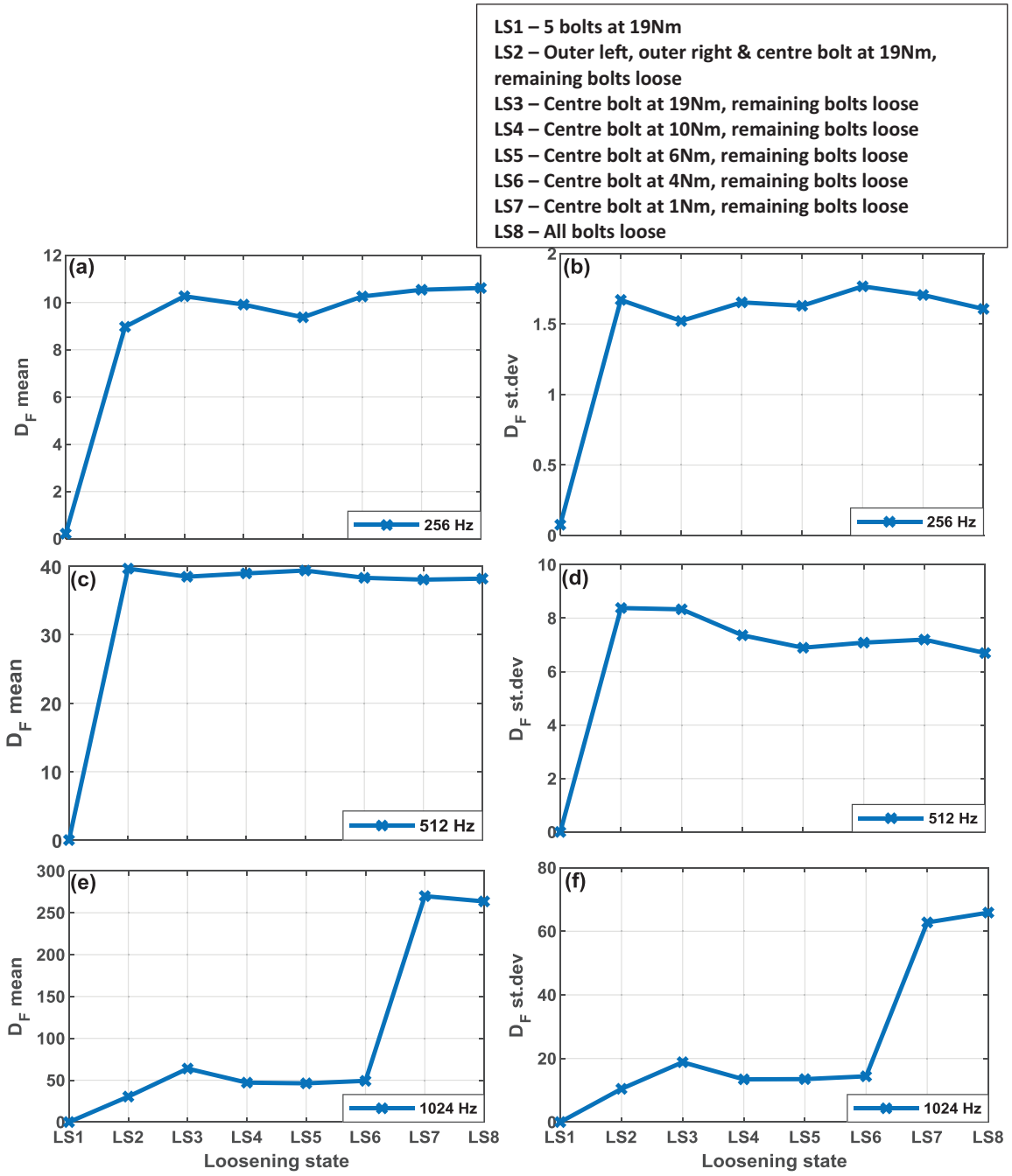

FIGURE 16 (a, c, e) Mean and (b, d, f) standard deviation of the damage characteristic parameter, $\boldsymbol{D_F}$ for various degree of structure loosening, sampled at 256, 512, and 1024 Hz and derived through the ARX model

than twice the frequency of interest is required. For wind turbine, the resonant frequency was found to be between 0.35 and 2 Hz [36] and consequently a minimum accelerometer sampling frequency of 0.7– 4 Hz is necessary for bolt joint detection through the methods outlined in this study. Such sampling rates are 2–3 order of magnitudes lower than those employed for experimental research [16, 22]. This could facilitate a bolt loosening detection system, built around low-cost microprocessors which read and process the accelerometer measurements and subsequently store or feed the result, at a similar acquisition rate to the turbine SCADA data for streamlined data agglomeration. However, there would be differences in the resonant frequency between different wind turbine models and components within the wind turbine such as the gearbox, all factors required to be considered for appropriate selection of the sampling rate of accelerometer measurements. For bolt joint looseness detection on different components or structures using the resonance frequency method, the resonance frequency which corresponds to the unloosened state or minimum tightening condition of the bolts is required to be determined, beyond which maintenance

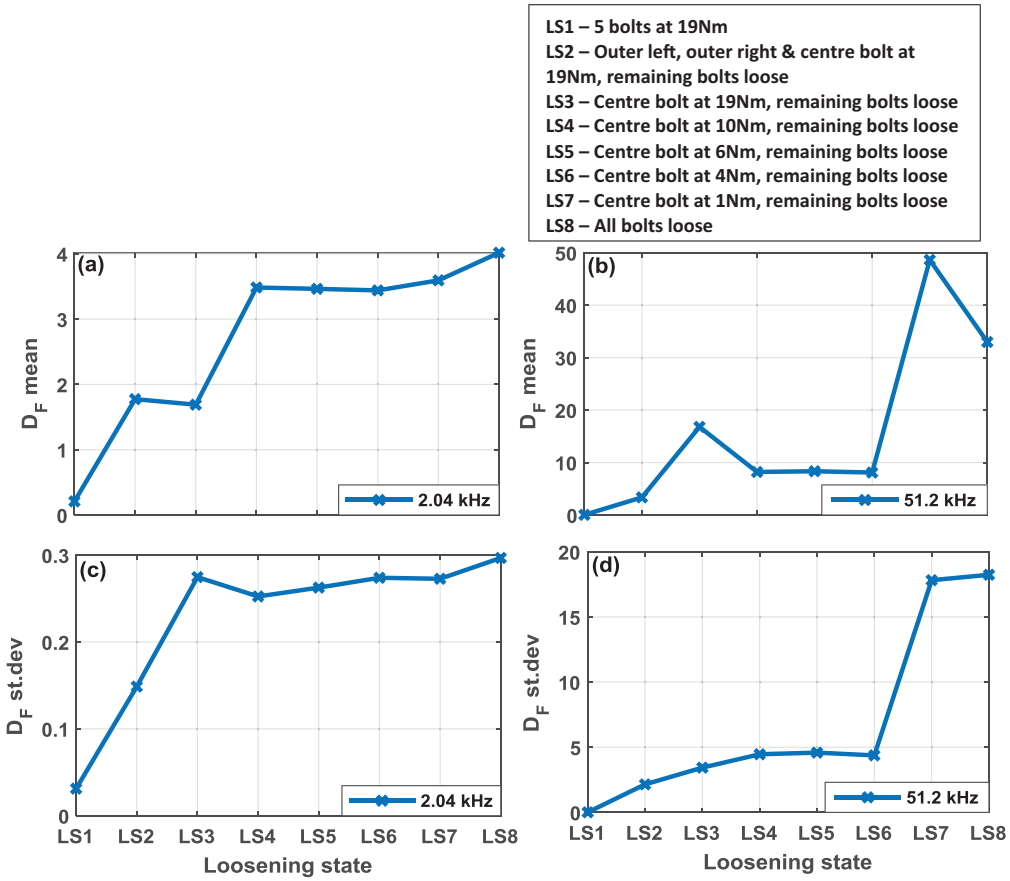

FIGURE 17 (a) and (b) Mean and (c) and (d) standard deviation of damage characteristic parameter, D_F for various degree of structure loosening, sampled at 2.04 and 51.2 kHz, derived through the AR-ARX model

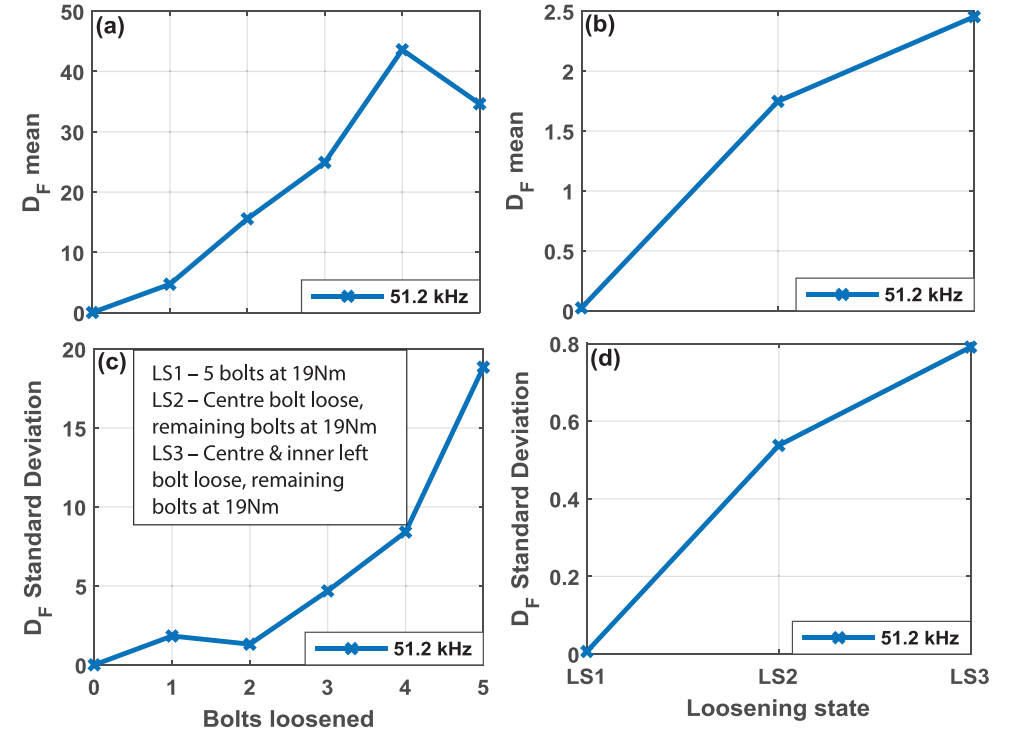

FIGURE 18 (a) and (b) Mean and (c) and (d) standard deviation of damage characteristic parameter, D_F for various degree of structure loosening, sampled at 51.2 kHz, derived through the AR-ARX model

is necessary to retighten the bolted joints. Conversely, for the regression methods, it is the upper limit for the mean and standard deviation of the damage characteristic parameter, D_F. This can be determined on-site prior during the installation of a new wind turbine, during a routine maintenance, or off-site through experimental testing using a replica. Vibration sensors should be positioned close to bolt joints that were of monitoring interest to maximise the proportion of signal measured from the bolt joints, thus reducing the occurrence of false detection. To further minimise instances of false detection, for every different sensor positioning configuration relative to the bolted joints, new regression models are required to be built and baseline mean, and standard deviation of the damage characteristic parameter D_F re-established.

5 | CONCLUSIONS

In this work, the feasibility of using low-sampled vibration signals for bolt joint tightness detection was investigated. Measurements were carried out on a specimen with an array of bolt joints on a test plate coupled to an electrodynamic shaker rig. Three detection methods were trialled and were successfully used to deduce bolt joint loosening from the accelerometer measurements, namely the resonant frequency and regression methods (ARX and AR-ARX).

Conclusions of this study are summarised below:

- Bolt resonant frequency and regression methods (ARX, AR-ARX) can be used to detect the loosening of bolt joints.
- In this study, a minimum sampling frequency of 1024 Hz was sufficient to allow for bolt joint looseness detection. The minimum sampling frequencies would be highly dependent on the resonant frequency of the structure.
- The resonant frequency method was not able to detect from an array of bolts the exact bolt, which was loosened, which with two regression methods (ARX, AR-ARX) were possible.
- The damage characteristic parameter, D_F computed from both ARX and AR-ARX regression methods were successfully used to provide an indication of bolt joint tightness, with the latter method requiring higher computational power.
- Since the resonant frequency of wind turbines are low (0.35–2 Hz), a minimum sampling rate of 0.7–4 Hz is sufficient for bolt joint looseness detection. This allow for the potential use of existing accelerometer instrumentations on wind turbines for bolt joint looseness detection as the measurements are usually sampled at a low rate ($< 10Hz$).

ACKNOWLEDGEMENTS

The authors would like to acknowledge the financial support of the Engineering and Physical Sciences Research Council for part funding this research through Rob Dwyer-Joyce's fellowship on *Tribo-Acoustic Sensors* EP/N016483/1. This project has also been carried out within the Powertrain Research Hub, PTRH co-funded by the Offshore Renewable Energy Catapult. The authors would like to acknowledge their help and support. The authors would also like to thank Dr. Ian Efremov for his advice and help.

CONFLICT OF INTEREST

The authors have declared no conflict of interest.

DATA AVAILABILITY STATEMENT

The data that support the findings of this study are available from the corresponding author upon reasonable request.

ORCID

Gary Nicholas https://orcid.org/0000-0002-0901-3276

REFERENCES

1. Miller, M., Johnson, C., Sonne, N., Mersch, J., Kuether, R., Smith, J., Ortiz, J., Castelluccio, G., Moore, K.: Bolt preload loss due to modal excitation of a C-beam structure. Conference Proceedings of the Society for Mechanics Series. (2020)
2. Zhang, M., Jiang, Y., Lee, C.: Finite element modelling of self-loosening of bolted joints. J. Mech. Des. 129(2), 218–226 (2007)
3. Junker, G.: New criteria for self-loosening of fasteners under vibration. SAE Trans. 78, 314–335 (1969)
4. Pai, N., Hess, D.: Experimental study of loosening of threaded fasteners due to dynamic shear loads. J. Sound Vib. 253(3), 585–602 (2002)
5. Pai, N., Hess, D.: Three-dimensional finite element analysis of threaded fastener loosening due to dynamic shear load. Eng. Fail. Anal. 9, 383–402 (2002)
6. Koch, D.: Beitrag zur numerischen Simulation des selbstta¨tigen Losdrehverhaltens von Schraubenverbindungen. PhD Thesis, University of Siegen (2012)
7. US Department of Energy: The importance of motor shaft alignment, energy tips: Motor systems. https://bit.ly/3eIwKLk (2014)
8. Pruftechnik Ltd: A practical guide to shaft alignment. https://bit.ly/3Bu66Q2 (2007)
9. Fisher, J., Struik, J.: Guide to Design Criteria for Bolted and Riveted Joints, 2nd ed. John Wiley & Sons, Hoboken, NJ (1987)
10. Bickford, J.: An Introduction to the Design and Behaviour of Bolted Joints, 3rd ed. CRC Press, Boca Raton, FL (1995)
11. Bickford, J., Nassar, S.: Handbook of Bolts and Bolted Joints, 1st ed. CRC Press, Boca Raton, FL (1998)
12. Eccles, W.: Tribological aspects of the self-loosening of threaded fasteners. PhD Thesis, University of Central Lancashire (2010)
13. Bickford, J.: Introduction to the Design and Behaviour of Bolted Joints: Non-Gasketed Joints, 4th ed. CRC Press, Boca Raton, FL (2007)
14. Bhalla, C.: Structural health monitoring by piezoimpedance transducers I: Modelling. J. Aerosp. Eng. 17(4), 154–165 (2004)
15. Rosiek, M., Martowicz, A., Uhl, T.: An overview of electromechanical impedance method for damage detection in mechanical structures. 6th European Workshop on Structural Health Monitoring. (2012)
16. Tanner, N., Wait, J., Farrar, C., Sohn, H.: Structural health monitoring using modular wireless sensors. J. Intell. Mater. Syst. Struct. 14(4), 43–56 (2003)
17. Milanese, A., Marzocca, P., Nichols, J., Seaver, M., Trickey, S.: Modelling and detection of joint loosening using output-only broad-band vibration data. Struct. Health Monitor. 7(4), 309–328 (2008)
18. He, K., Zhu, W.: Detecting loosening of bolted connections in a pipeline using changes in natural frequencies. J. Vib. Acoust. 136(3), 034503 (2014)
19. Wang, T., Song, G., Wang, Z., Li, Y.: Proof-of-concept study of monitoring bolt connection status using a piezoelectric based active sensing method. Smart Mater. Struct. 22, 087001 (2002)
20. Chakim, S., Corneloup, G., Lillamand, I., Walaszek, H.: Combination of longitudinal and transverse ultrasonic waves for in situ control of the tightening of bolts. J. Pressure Vessel Technol. 129(3), 383–390 (2007)
21. Zhang, Z., Liu, M., Su, Z., Xiao, Y.: Evaluation of bolt loosening using a hybrid approach based on contact acoustic nonlinearity. The 19th World Conference on Non-Destructive Testing. (2016)

22. Dong, G., Zhao, F., Zhang, X.: Experimental study on monitoring the bolt group looseness in a clamping support structure model. Adv. Mech. Eng. 9(3), 1–12 (2017)
23. Park, J., Huynh, T., Choi, S., Kim, J.: Vision-based technique for bolt-loosening detection in wind turbine tower. Wind Struct. 21(6), 709–726 (2015)
24. Huynh, T., Park, J., Jung, H., Kim, J.: Quasi-autonomous bolt-loosening detection method using vision-based deep learning and image processing. Autom. Constr. 105, 102844 (2019)
25. Cha, Y., You, K., Choi, W.: Vision-based detection of loosened bolts using the Hough transform and support vector machines. Autom. Constr. 71, 181–188 (2016)
26. Yu, Y., Liu, Y., Chen, J., Jiang, D., Zhuang, Z., Wu, X.: Detection method for bolted connection looseness at small angles of timber structures based on deep learning. Sensors 21, 3106 (2021)
27. Huang, Y., Liu, L., Yueng, T., Hung, Y.: Real-time monitoring of clamping force of a bolted joint by use of automatic digital image correlation. Opt. Laser Technol. 41, 408–414 (2009)
28. Nikravesh, S., Goudarzi, M.: A review paper on looseness detection methods in bolted structures. Latin Amer. J. Solids Struct. 14(12), 2153–2176 (2017)
29. Huang, J., Liu, J., Gong, H., Deng, X.: A comprehensive review of loosening detection methods for threaded fasteners. Mech. Syst. Sig. Process. 168, 108652 (2022)
30. Miao, R., Shen, R., Zhang, S., Xue, S.: A review of bolt tightening force measurement and looseness detection. Sensors 20, 3165 (2020)
31. Nguyen, T., Huynh, T., Yi, J., Kim, J.: Hybrid bolt-loosening detection in wind turbine tower structures by vibration and impedance responses. Wind Struct. 24(4), 385–403 (2017)
32. Sohn, H., Farrar, C., Hunter, N., Worden, K.: Structural health monitoring using statistical pattern recognition techniques. J. Dynam. Syst. Meas. Control 123(4), 706–711 (2001)
33. Sohn, H., Farrar, C.: Damage diagnosis using time series analysis of vibration signals. Smart Mater. Struct. 10, 446–451 (2001)
34. Ljung, L.: System Identification, Theory for Use. Prentice-Hall, Hoboken, NJ (1987)
35. Ljung, L.: System Identification Toolbox User's Guides. The MathWorks, Natick, MA (2000)
36. Devriendt, C., Weijtjens, W., El-Kafafy, M., Sitter, G.: Monitoring resonant frequencies and damping values of an offshore wind turbine in parked conditions. IET Renew. Power Gener. 8(4), 433–441 (2014)

How to cite this article: Nicholas, G., Mills, R., Song, W., Lee, H., Dwyer-Joyce, R.: Feasibility of using low-sampled accelerometer measurements for bolt joint looseness detection. IET Renew. Power Gener. 1–16 (2022). https://doi.org/10.1049/rpg2.12512